

# Comparative analysis of multiple mathematical models for prediction of consistency and compressive strength of ultra-high performance concrete

Alireza Habibi<sup>\*1</sup>, Meysam Mollazadeh<sup>2a</sup>, Aryan Bazrafkan<sup>3b</sup> and Naida Ademovic<sup>4c</sup>

<sup>1</sup>Department of Civil Engineering, Shahed University, Tehran, Iran

<sup>2</sup>Department of Civil Engineering, Kurdistan University, Sanandaj, Iran

<sup>3</sup>Department of Civil Engineering, Bijar Branch, Islamic Azad University, Bijar, Iran

<sup>4</sup>Faculty of Civil Engineering Sarajevo, University of Sarajevo, Bosnia and Herzegovina

(Received March 19, 2023, Revised October 29, 2023, Accepted November 16, 2023)

**Abstract.** Although some prediction models have successfully developed for ultra-high performance concrete (UHPC), they do not provide insights and explicit relations between all constituents and its consistency, and compressive strength. In the present study, based on the experimental results, several mathematical models have been evaluated to predict the consistency and the 28-day compressive strength of UHPC. The models used were Linear, Logarithmic, Inverse, Power, Compound, Quadratic, Cubic, Mixed, Sinusoidal and Cosine equations. The applicability and accuracy of these models were investigated using experimental data, which were collected from literature. The comparisons between the models and the experimental results confirm that the majority of models give acceptable prediction with a high accuracy and trivial error rates, except Linear, Mixed, Sinusoidal and Cosine equations. The assessment of the models using numerical methods revealed that the Quadratic and Inverse equations based models provide the highest predictability of the compressive strength at 28 days and consistency, respectively. Hence, they can be used as a reliable tool in mixture design of the UHPC.

**Keywords:** compressive strength; consistency; mathematical model; ultra high performance concrete

## 1. Introduction

Ultra-high performance concrete (UHPC) is described by its high compressive strength, high toughness, dense material, low capillary porosity, and long-term durability (Meng *et al.* 2016, Meng *et al.* 2018). Given the high mechanical properties, UHPC has been used in structures for construction (Wang *et al.* 2021, Liu *et al.* 2019, Bao *et al.* 2017), repair (Zmetra *et al.* 2017, Du *et al.* 2021, Cheng *et al.* 2021), and rehabilitation (Guo *et al.* 2021, Qi *et al.* 2021, Yin *et al.* 2017). The mechanical properties of UHPC such as the compressive strength and slump flow are a highly

---

\*Corresponding author, Professor, E-mail: ar.habibi@shahed.ac.ir

<sup>a</sup>M.Sc., E-mail: meysam\_mollazadeh@yahoo.com

<sup>b</sup>Assistant Professor, E-mail: aryan\_bazrafkan@iaubijar.ac.ir

<sup>c</sup>Associate Professor, E-mail: naida.ademovic@gf.unsa.ba

nonlinear functions of its constituents. The significance of expert frameworks for predicting the compressive strength and slump flow of UHPC is greatly distinguished in material technology.

The effect of various constituent materials on compressive, flexural, and tensile strengths, fiber-matrix bond, rheological, applicable flow models, measurement techniques and errors associated with the interpretation of rheological measurements was investigated. In addition, the rheological properties requirements of UHPC and strategies to control rheology were considered. It was observed that the silica fume content, ranging from 10% to 15%, by mass of cementitious materials, established the highest fiber-matrix bond, flexural and tensile properties. Such silica fume content was found to result in lower viscosity and more uniformly distributed fibers as determined by image analysis. Also, the addition of steel wool in steel fiber-reinforced UHPC Compared to control UHPC with no steel wool, produced significant improvement in the fiber-matrix bond and mechanical properties of UHPC. Surrounding the steel fibers with steel wool, enhanced the bond between steel fibers and a UHPC matrix (Khayat *et al.* 2019, Wu *et al.* 2019, Regalwar *et al.* 2020). Some researchers developed a numerical study with experimental work to predict several mechanical properties of UHPC. For instance, a numerical study comparing to tie interaction model was investigated to estimate the load capacity of structures where UHPC is joined as an overlay and normal strength concrete as substrate section. It was shown that employing the numerical model provided a better prediction of the failure loads when compared to the tied model. Moreover, Impact responses of UHPC targets with 3 Vol-% steel fibers and UHPC targets with ultra-high molecular weight polyethylene (UHMWPE) fibers were investigated subjected to high-velocity projectile penetration. The experimental results were compared with the numerical results in terms of the depth of penetration and crater diameter as well as projectile abrasions and damages (Liu *et al.* 2018, Farzad *et al.* 2019).

Modeling UHPC in the fresh and hardened state is usually a valuable aim and a difficult task at the identical time. This task is difficult due to the non-linearity of UHPC. The heterogeneity of UHPC and the large number of factors affecting its properties are the sources of this non-linearity. A considerable number of studies concerning the prediction of UHPC properties have been carried out, and the plenty of improved prediction techniques were proposed including empirical or computational modeling and statistical techniques. Many modeling methods were used to predict the mechanical properties (compressive, flexural, and tensile strengths in particular) of UHPC, including the artificial neural network (Abellán-García 2020, Bui *et al.* 2018, Al-Shamiri *et al.* 2019, Ghafari *et al.* 2015, Qu *et al.* 2017), and regression models (Wu *et al.* 2019, Dao *et al.* 2020, Nguyen *et al.* 2022). Some methods were proposed based on the artificial neural network, which was trained using different data to estimate the compressive strength of UHPC with several mix design factors (Abellán-García 2020, Qu *et al.* 2017, Ghafari *et al.* 2015). These experimental data-based models considered the effects of constituent materials such as steel fiber content and shape, silica fume, quartz flour, and superplasticizer quantities on different mechanical properties of UHPC. Some prediction models were presented to predict the compressive, flexural, and tensile strengths of these type of concretes. However, no study was investigated the same for using the silica fume, quartz flour, and steel fibers together as ingredients.

In this paper, a comprehensive 53 mix designs of UHPC with 7 ingredients, which are collected from literature (Ghafari *et al.* 2015) have been used to evaluate the mathematical models to predict its slump flow, and 28-day compressive strength. Regression models including Linear, Logarithmic, Inverse, Power, Compound, Quadratic, Cubic, Mixed, Sinusoidal and Cosine equations are evaluated to provide explicit equations between ingredients and mechanical properties of UHPC. These models were justified using statistical parameters such as  $R^2$ , and Error

percentage with experimental observations. The lowest error percentage of 7, and 9.4, and the  $R^2$  of 0.97, and 0.92 are obtained for Inverse-type 2, and Quadratic-type 2 regression models in predicting slump flow, and 28-day compressive strength, respectively. The present results not only show better performance with those from previous study in terms of error%, and  $R^2$ , but also have explicit relations of slump flow, and compressive strength with 7 input ingredients.

## 2. Data collection

Creating a general and reliable dataset is a vital step in developing mathematical models. For this purpose, a comprehensive literature review was carried out to collect data from published research papers. Different cementitious materials, fine and ultra-fine aggregates, shapes and types of fibers, fillers, superplasticizer, and etc... have been incorporated in UHPC to improve its consistency and strength. Therefore, there are many input features that could be considered for a mathematical model to predict the slump flow, and the compressive strength of UHPC. Considering the numerous experimental studies that used such materials in UHPC mixture designs, along with several curing regimes, a large dataset comprising various mixture components was collected. Thus, a dataset consisting of 53 mix designs, 159 test observations, and 7 input features were assigned to develop the prediction models. The following constituents have been used in extracted data:

- Ordinary Portland cement type I 52.5 R,
- siliceous sand (SA), with maximum aggregates' size of 0.6 mm,
- silica fume,
- Quartz flour with particles' size lower than 10  $\mu\text{m}$  used as micro filler
- polycarboxylate ether based superplasticizers,
- DRAMIX steel micro fibers, with diameter/length of 0.2/0.15 mm

Table 1 reports the mix proportions, and Figs. 1 and 2 present the slump flow, and the 28-day compressive strength results used in this study, respectively. (Ghafari *et al.* 2015). As illustrated in Fig. 1, minimum and maximum values of the slump flows are 171 mm (related to design mix no. 33) and 234 mm (related to design mix no. 47). Fig. 2 shows that minimum and maximum values of the compressive strength are 90 MPa and 200 MPa, which are related to design mix nos. 9 and 43, respectively. Mix 9 contains  $w/C = 0.26$ , silica fume=36 Kg, quartz flour=297 Kg, superplasticizer=36 Kg, without the steel fibers, while mix 43 contains  $w/C = 0.23$ , silica fume=36 Kg, quartz flour=243 Kg, superplasticizer=36 Kg, with steel fibers=160 Kg. This means that in mix 43, water to cement ratio have been decreased and the steel fibers have been increased respect to mix 9.

Table 1 Mix proportions considered in dataset extracted from literature. (Ghafari *et al.* 2015)

Design No.	Water (Kg)	Cement (Kg)	Sand (Kg)	Silica Fume (Kg)	Quartz Flour (Kg)	Super Plasticizer (Kg)	Steel Fibers (Kg)
1	190	800	844	48	216	36	80
2	200	896	765	54	216	36	0
3	200	896	739	42	324	36	0
4	210	832	686	54	297	48	0
5	190	800	844	48	216	36	80
6	190	800	924	48	189	36	0

Table 1 Continued

Design No.	Water (Kg)	Cement (Kg)	Sand (Kg)	Silica Fume (Kg)	Quartz Flour (Kg)	Super Plasticizer (Kg)	Steel Fibers (Kg)
7	190	800	924	36	243	36	0
8	180	736	924	48	243	36	80
9	200	768	897	36	297	36	0
10	200	768	871	48	243	36	0
11	200	1088	897	36	0	36	0
12	200	1024	871	48	0	36	0
13	200	960	897	36	108	36	0
14	180	704	1029	36	243	36	0
15	200	832	897	48	162	36	0
16	180	640	1161	42	189	36	0
17	200	864	792	42	216	48	160
18	180	704	950	60	216	36	0
19	180	704	950	60	216	36	0
20	170	704	976	48	270	36	0
21	200	864	844	48	162	36	0
22	200	928	818	48	162	36	0
23	200	800	818	48	243	36	80
24	200	896	897	48	108	36	0
25	200	800	792	48	243	36	160
26	200	832	897	48	162	36	0
27	200	768	897	54	189	36	0
28	200	768	897	60	162	36	0
29	200	768	897	72	108	36	0
30	160	672	1029	48	270	36	0
31	200	768	897	42	243	36	0
32	190	800	844	48	216	36	80
33	180	864	818	48	270	36	0
34	190	864	818	42	270	36	0
35	190	800	871	48	243	36	0
36	190	768	897	36	273	36	160
37	190	864	818	42	270	36	0
38	180	736	924	48	243	36	80
39	160	672	1029	48	270	36	0
40	200	800	818	48	243	36	80
41	160	704	1082	36	243	36	0
42	190	736	924	54	216	36	0
43	180	768	924	36	243	36	160
44	180	736	950	48	243	36	0
45	210	800	792	48	243	36	160
46	180	768	871	48	243	36	0
47	200	768	879	36	270	36	0
48	200	864	792	42	216	48	160
49	180	800	950	48	162	36	160
50	210	800	792	48	243	36	160
51	190	768	844	48	243	36	80
52	200	768	897	66	135	36	0
53	180	768	871	42	243	36	160

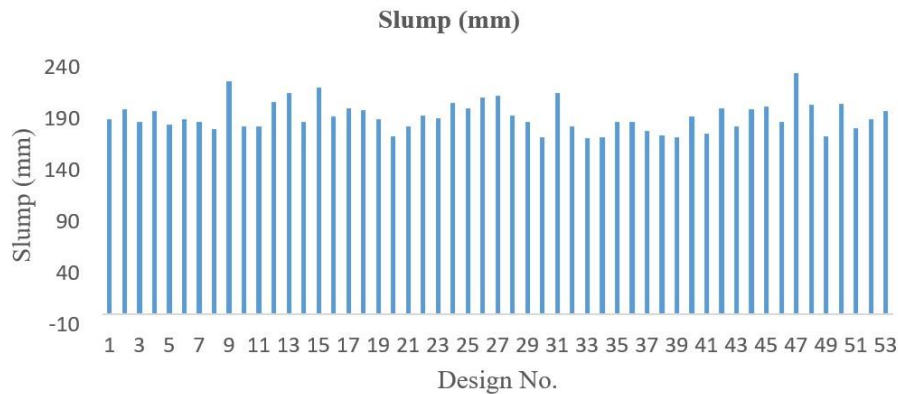


Fig. 1 Results of the slump flow tests for the mixes (Ghafari *et al.* 2015)

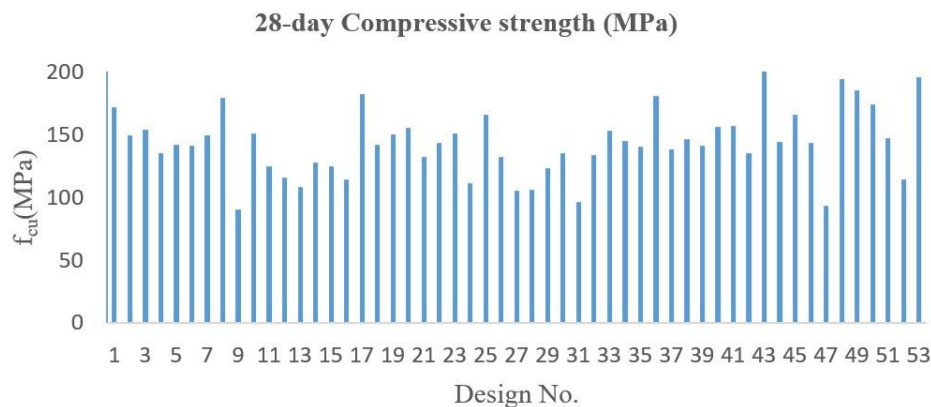


Fig. 2 Results of the 28-day compressive strength tests for the mixes (Ghafari *et al.* 2015)

### 3. Prediction modelling

Sixteen multivariable regression models have been developed by including empirical and statistical techniques to evaluate the accuracy of 28-day compressive strength and slump flow of UHPC predictions. The quantities of cement, sand, silica fume, quartz flour, water, superplasticizer and steel fibers have been considered as design variables to generate the models.

#### 3.1 UHPC compressive strength and slump flow prediction models

UHPC strength and slump flow are influenced by many factors such as water to cement ratio, quantities of silica fume, quartz flour, steel fibers, and superplasticizer dosage. This research represented several regression models that can help to predict the 28-day compressive strength and the rate of slump flow for different UHPC mix designs.

Based on design parameters and statistical properties, various mathematical patterns including linear, logarithmic, inverse, power, compound, quadratic, cubic and linear with inverse mixed equations based models were adopted to predict the UHPC 28-day compressive strength and slump flow. The models are expressed in Eqs. 1 to 48 which mathematical features of the models

are described below.

$x_1, x_2, x_3, x_4, x_5, x_6, x_7$  are cement, sand, silica fume, quartz flour, water, superplasticizer and steel fibers, respectively. Each relation contains some constant coefficients ( $b_0$ - $b_{31}$ ) which are determined by the least-square method. This method is used to minimize the error between predicted response by the relation and measured response by the test. Regression are performed on the compressive strength and the slump flow applying the proposed models and considering seven variables  $x_1, x_2, x_3, x_4, x_5, x_6$  and  $x_7$  as the independent variables.

### 3.1.1 Linear equation based model

$$f_1(x) = b_0 + b_1x_1 + b_2x_2 + b_3x_3 + b_4x_4 + b_5x_5 + b_6x_6 + b_7x_7 \quad (1)$$

$$f_{cm} = -66.8 + 0.25x_1 + 0.08x_2 + 1.3x_3 + 0.23x_4 - 1.1x_5 + 0.69x_6 + 0.37x_7 \quad (2)$$

$$Slm = 282.2 + 0.17x_1 + 0.068x_2 + 1.1x_3 + 0.14x_4 - 0.97x_5 + 0.42x_6 + 0.08x_7 \quad (3)$$

### 3.1.2 Logarithmic equation based model

$$f_2(x) = b_0 + b_1 \ln(x_1) + b_2 \ln(x_2) + b_3 \ln(x_3) + b_4 \ln(x_4) + b_5 \ln(x_5) + b_6 \ln(x_6) + b_7 \ln(x_7) \quad (4)$$

$$f_{cm} = -7209.1 + 731.9 \ln(x_1) + 317.3 \ln(x_2) + 157 \ln(x_3) + 222.8 \ln(x_4) - 321.9 \ln(x_5) - 17.8 \ln(x_6) + 62.9 \ln(x_7) \quad (5)$$

$$Slm = -3541.6 + 461.4 \ln(x_1) + 40.69 \ln(x_2) + 117.8 \ln(x_3) + 152 \ln(x_4) - 171 \ln(x_5) - 36.1 \ln(x_6) + 28.1 \ln(x_7) \quad (6)$$

### 3.1.3 Inverse equation based model

#### 3.1.3.1 Inverse equation based model -Type one

$$f_3(x) = b_0 + \frac{b_1}{x_1} + \frac{b_2}{x_2} + \frac{b_3}{x_3} + \frac{b_4}{x_4} + \frac{b_5}{x_5} + \frac{b_6}{x_6} + \frac{b_7}{x_7} \quad (7)$$

$$f_{cm} = 1563.8 - \frac{615358.5}{x_1} - \frac{373440.2}{x_2} - \frac{7164.3}{x_3} - \frac{49518.5}{x_4} + \frac{49084.9}{x_5} + \frac{366.6}{x_6} - \frac{7257.7}{x_7} \quad (8)$$

$$Slm = 945 - \frac{395360}{x_1} - \frac{104620}{x_2} - \frac{5322.6}{x_3} - \frac{34124.4}{x_4} + \frac{24558}{x_5} + \frac{1366}{x_6} - \frac{3268.5}{x_7} \quad (9)$$

#### 3.1.3.2 Inverse equation based model -Type two

$$f_4(x) = b_0 + \frac{b_1}{x_1} + \frac{b_2}{x_2} + \frac{b_3}{x_3} + \frac{b_4}{x_4} + \frac{b_5}{x_5} + \frac{b_6}{x_6} + \frac{b_7}{x_7} + \frac{b_8}{x_5} + \frac{b_9}{x_4} + \frac{b_{10}}{x_4 + x_3 + x_1} \quad (10)$$

$$f_{cm} = 231 - \frac{93308}{x_1} - \frac{32181.3}{x_2} - \frac{1346.8}{x_3} - \frac{14.098}{x_4} + \frac{34979.7}{x_5} - \frac{2721}{x_6} - \frac{0.378}{x_7} + \frac{10.25}{x_5} + \frac{0.016}{x_4} - \frac{2658192.55}{x_4 + x_3 + x_1} \quad (11)$$

$$Slm = 173 + \frac{90988.6}{x_1} - \frac{52927.9}{x_2} - \frac{4767.7}{x_3} - \frac{249110.8}{x_4} + \frac{59193.9}{x_5} + \frac{3910.3}{x_6} - \frac{3112.4}{x_7} - \frac{58}{x_1} + \frac{270}{x_1} + \frac{14812775.58}{\frac{x_5}{x_4+x_3+x_1}} \quad (12)$$

### 3.1.3.3 Inverse equation based model -Type three

$$f_5(x) = b_0 + \frac{b_1}{x_1} + \frac{b_2}{x_2} + \frac{b_3}{x_3} + \frac{b_4}{x_4} + \frac{b_5}{x_5} + \frac{b_6}{x_6} + \frac{b_7}{x_7} + \frac{b_8}{x_5} + \frac{b_9}{x_1} + \frac{b_{10}}{\frac{x_5}{x_4+x_3+x_1}} + b_{11}x_1x_2x_3x_4x_5x_6x_7 \quad (13)$$

$$f_{cm} = 232 - \frac{93308}{x_1} - \frac{32181}{x_2} - \frac{1347}{x_3} - \frac{14}{x_4} + \frac{34979}{x_5} - \frac{2721}{x_6} - \frac{0.378}{x_7} + \frac{11}{x_5} + \frac{0.016}{x_1} - \frac{2658192}{\frac{x_5}{x_4+x_3+x_1}} - 2.68 \times 10^{-0.14}x_1x_2x_3x_4x_5x_6x_7 \quad (14)$$

$$Slm = 4160 - \frac{3677141}{x_1} + \frac{20783}{x_2} + \frac{2058}{x_3} - \frac{2487983}{x_4} + \frac{2930348}{x_5} + \frac{10527}{x_6} - \frac{15219}{x_7} - \frac{3738}{x_1} + \frac{3154}{x_1} - \frac{330211}{\frac{x_5}{x_4+x_3+x_1}} - 2.7 \times 10^{-0.14}x_1x_2x_3x_4x_5x_6x_7 \quad (15)$$

### 3.1.4 Power equation based model

#### 3.1.4.1 Power equation based model -Type one

$$f_6(x) = b_0x_1^{b_1}x_2^{b_2}x_3^{b_3}x_4^{b_4}x_5^{b_5}x_6^{b_6}x_7^{b_7} \quad (16)$$

$$f_{cm} = 7.255 \times 10^{-6}x_1^{1.76}x_2^{0.78}x_3^{0.39}x_4^{0.613}x_5^{1.3}x_6^{0.12}x_7^{0.31} \quad (17)$$

$$Slm = 0.002x_1^{1.7}x_2^{0.15}x_3^{0.45}x_4^{0.6}x_5^{0.76}x_6^{0.14}x_7^{0.13} \quad (18)$$

#### 3.1.4.2 Power equation based model -Type two

$$f_7(x) = b_0x_1^{b_1}x_2^{b_2}x_3^{b_3}x_4^{b_4}x_5^{b_5}x_6^{b_6}x_7^{b_7}\left(\frac{x_5}{x_1}\right)^{b_8}\left(\frac{x_4}{x_1}\right)^{b_9}\left(\frac{x_5}{x_1+x_4+x_3}\right)^{b_{10}} \quad (19)$$

$$f_{cm} = 2.105x_1^{3.881}x_2^{2.72}x_3^{2.40}x_4^{5.40}x_5^{3.5}x_6^{-0.24}x_7^{0.377}\left(\frac{x_5}{x_1}\right)^{4.805}\left(\frac{x_4}{x_1}\right)^{4.086}\left(\frac{x_5}{x_1+x_4+x_3}\right)^{-10.036} \quad (20)$$

$$Slm = 1.470x_1^{-2.17}x_2^{-0.128}x_3^{0.16}x_4^{2.524}x_5^{3.97}x_6^{-0.136}x_7^{0.140}\left(\frac{x_5}{x_1}\right)^{-5.03}\left(\frac{x_4}{x_1}\right)^{0.696}\left(\frac{x_5}{x_1+x_4+x_3}\right)^{3.14} \quad (21)$$

#### 3.1.4.3 Power equation based model -Type three

$$f_8(x) = b_0x_1^{b_1}x_2^{b_2}x_3^{b_3}x_4^{b_4}x_5^{b_5}x_6^{b_6}x_7^{b_7} + b_8x_1x_2x_3x_4x_5x_6x_7 \quad (22)$$

$$f_{cm} = x_1^{1.8}x_2^{0.78}x_3^{0.42}x_4^{0.610}x_5^{-1.9}x_6^{0.12}x_7^{0.38} + 8.2x_1x_2x_3x_4x_5x_6 \quad (23)$$

$$Slm = 0.006x_1^{1.8}x_2^{-0.18}x_3^{0.50}x_4^{0.6}x_5^{-0.76}x_6^{-0.14}x_7^{0.13} + 6.25x_1x_2x_3x_4x_5x_6 \quad (24)$$

### 3.1.5 Compound equation based model

$$f_9(x) = b_0 b_1^{x_1} b_2^{x_2} b_3^{x_3} b_4^{x_4} b_5^{x_5} b_6^{x_6} b_7^{x_7} \quad (25)$$

$$f_{cm} = 8.728 \times 1.003^{x_1} \times 1.001^{x_2} \times 1.011^{x_3} \times 1.003^{x_4} \times 0.992^{x_5} \times 1.001^{x_6} \times 1.003^{x_7} \quad (26)$$

$$Slm = 31.36 \times 1.002^{x_1} \times 1.00^{x_2} \times 1.011^{x_3} \times 1.003^{x_4} \times 0.995^{x_5} \times 0.966^{x_6} \times 1.02^{x_7} \quad (27)$$

### 3.1.6 Quadratic equation based model

#### 3.1.6.1 Quadratic equation based model -Type one

$$f_{10}(x) = b_0 + b_1 x_1 + b_2 x_2 + b_3 x_3 + b_4 x_4 + b_5 x_5 + b_6 x_6 + b_7 x_7 + b_8 x_1 x_2 + b_9 x_1 x_3 + b_{10} x_1 x_4 + b_{11} x_1 x_5 + b_{12} x_1 x_6 + b_{13} x_1 x_7 + b_{14} x_2 x_3 + b_{15} x_2 x_4 + b_{16} x_2 x_5 + b_{17} x_2 x_6 + b_{18} x_2 x_7 + b_{19} x_3 x_4 + b_{20} x_3 x_5 + b_{21} x_3 x_6 + b_{22} x_3 x_7 + b_{23} x_4 x_5 + b_{24} x_4 x_6 + b_{25} x_4 x_7 + b_{26} x_5 x_6 + b_{27} x_5 x_7 + b_{28} x_6 x_7 \quad (28)$$

$$f_{cm} = 21403302 + 20413x_1 - 4026.6x_2 - 383860x_3 - 155621x_4 + 149106x_5 - 594238x_6 - 99670x_7 + 0.001x_1x_2 + 0.003x_1x_3 + 0.001x_1x_4 + 0.026x_1x_5 - 567.2x_1x_6 - 0.002x_1x_7 + 0.006x_2x_3 + 0.001x_2x_4 + 0.018x_2x_5 + 111.8x_2x_6 + 0.001x_2x_7 + 0.004x_3x_4 + 0.167x_3x_5 + 10662x_3x_6 - 0.013x_3x_7 + 0.036x_4x_5 + 4322x_4x_6 - 0.001x_4x_7 - 4143.3x_5x_6 + 0.010x_5x_7 + 2768.7x_6x_7 \quad (29)$$

$$Slm = -6678237 + 28345x_1 + 82.8x_2 - 280367x_3 - 141053x_4 + 190824x_5 + 185450x_6 - 86222x_7 + 0.001x_1x_2 + 0.10x_1x_3 + 1.296x_1x_4 + 0.001x_1x_5 - 787.4x_1x_6 - 0.007x_1x_7 - 0.011x_2x_3 - 0.001x_2x_4 - 0.007x_2x_5 - 2.271x_2x_6 - 0.005x_2x_7 - 0.001x_3x_4 - 0.141x_3x_5 + 7788.8x_3x_6 - 0.037x_3x_7 + 0.001x_4x_5 + 3918.2x_4x_6 - 0.007x_4x_7 - 5300.3x_5x_6 - 0.01x_5x_7 + 2395.8x_6x_7 \quad (30)$$

#### 3.1.6.2 Quadratic equation based model -Type two

$$f_{11}(x) = b_0 + b_1 x_1 + b_2 x_2 + b_3 x_3 + b_4 x_4 + b_5 x_5 + b_6 x_6 + b_7 x_7 + b_8 x_1 x_2 + b_9 x_1 x_3 + b_{10} x_1 x_4 + b_{11} x_1 x_5 + b_{12} x_1 x_6 + b_{13} x_1 x_7 + b_{14} x_2 x_3 + b_{15} x_2 x_4 + b_{16} x_2 x_5 + b_{17} x_2 x_6 + b_{18} x_2 x_7 + b_{19} x_3 x_4 + b_{20} x_3 x_5 + b_{21} x_3 x_6 + b_{22} x_3 x_7 + b_{23} x_4 x_5 + b_{24} x_4 x_6 + b_{25} x_4 x_7 + b_{26} x_5 x_6 + b_{27} x_5 x_7 + b_{28} x_6 x_7 + b_{29} \left(\frac{x_5}{x_1}\right) + b_{30} \left(\frac{x_4}{x_1}\right) + b_{31} \left(\frac{x_5}{x_1+x_4+x_3}\right) \quad (31)$$

$$f_{cm} = -458894 + 34564x_1 + 661.4x_2 + 2980338x_3 - 835917x_4 + 278927x_5 + 12960x_6 - 189576x_7 + 0.003x_1x_2 + 0.014x_1x_3 - 0.012x_1x_4 + 0.043x_1x_5 - 960.3x_1x_6 - 0.008x_1x_7 - 0.006x_2x_3 + 0.001x_2x_4 - 18.4x_2x_6 - 0.004x_2x_7 - 0.005x_3x_4 - 0.041x_3x_5 - 82787x_3x_6 - 0.035x_3x_7 + 0.011x_4x_5 + 23220x_4x_6 - 0.008x_4x_7 - 7749.5x_5x_6 + 0.010x_5x_7 + 5266.3x_6x_7 + 11628 \left(\frac{x_5}{x_1}\right) - 11487 \left(\frac{x_4}{x_1}\right) - 351.5 \left(\frac{x_5}{x_1+x_4+x_3}\right) \quad (32)$$

$$Slm = 69403572 - 200306x_1 - 197.77x_2 - 955594x_3 + 519002x_4 - 24643x_5 - 1927570x_6 + 229739x_7 - 0.002x_1x_2 - 0.005x_1x_3 - 0.006x_1x_4 + 0.038x_1x_5 + 5563.7x_1x_6 - 0.009x_2x_3 - 0.00x_2x_4 + 0.045x_2x_5 + 5.33x_2x_6 - 0.003x_2x_7 - 0.001x_3x_4 - 0.076x_3x_5 + 26544x_3x_6 - 0.009x_3x_7 - 0.076x_4x_5 - 14417x_4x_6 - 683.1x_5x_6 - 0.008x_5x_7 - 6381.5x_6x_7 + 9926.7 \left(\frac{x_5}{x_1}\right) - 2158.2 \left(\frac{x_4}{x_1}\right) + 909.4 \left(\frac{x_5}{x_1+x_4+x_3}\right) \quad (33)$$

### 3.1.7 Cubic equation based model

$$f_{12}(x) = b_0 + b_1x_1 + b_2x_2 + b_3x_3 + b_4x_4 + b_5x_5 + b_6x_6 + b_7x_7 + b_8x_1^2 + b_9x_2^2 + b_{10}x_3^2 + b_{11}x_4^2 + b_{12}x_5^2 + b_{13}x_6^2 + b_{14}x_7^2 + b_{15}x_1^3 + b_{16}x_2^3 + b_{17}x_3^3 + b_{18}x_4^3 + b_{19}x_5^3 + b_{20}x_6^3 + b_{21}x_7^3 \quad (34)$$

$$f_{cm} = 1 - 3.2x_1 + 2.1x_2 + 1.6x_3 - 0.26x_4 + 1.6x_5 + 2.1x_6 + 3679944856x_7 + 0.004x_1^2 - 0.003x_2^2 - 0.014x_3^2 + 0.02x_4^2 - 0.016x_5^2 - 0.724x_6^2 - 6898966x_7^2 - 1.951x_1^3 + 1.001x_2^3 + 3.069x_3^3 - 3.354x_4^3 + 2.35x_5^3 - 0.12x_6^3 + 28746x_7^3 \quad (35)$$

$$Slm = 3.85 - 4.6x_1 + 2.2x_2 + 5.6x_3 - 0.46x_4 + 1.8x_5 + 2.3x_6 + 2579988856x_7 + 0.003x_1^2 - 0.002x_2^2 - 0.015x_3^2 + 0.22x_4^2 - 0.017x_5^2 - 0.734x_6^2 - 7568966x_7^2 - 1.551x_1^3 + 1.021x_2^3 + 4.079x_3^3 - 4.254x_4^3 + 2.55x_5^3 - 0.22x_6^3 + 18736x_7^3 \quad (36)$$

### 3.1.8 Linear with Inverse mixed equation based model

#### 3.1.8.1 Linear with type one -Inverse mixed equation based model

$$f_{13}(x) = b_0 + b_1x_1 + \frac{b_2}{x_1} + b_3x_2 + \frac{b_4}{x_2} + b_5x_3 + \frac{b_6}{x_3} + b_7x_4 + \frac{b_8}{x_4} + b_9x_5 + \frac{b_{10}}{x_5} + b_{11}x_6 + \frac{b_{12}}{x_6} + b_{13}x_7 + \frac{b_{14}}{x_7} \quad (37)$$

$$f_{cm} = 707926 - 0.1x_1 - \frac{200492}{x_1} - 0.14x_2 + \frac{0.047}{x_2} + 0.35x_3 + \frac{247872}{x_3} + 0.7x_4 - \frac{852.4}{x_4} - 0.48x_5 - \frac{0.176}{x_5} - 8414x_6 - \frac{2.5}{x_6} + 66426x_7 - \frac{5471060}{x_7} \quad (38)$$

$$Slm = 74882 - 16.4x_1 + \frac{8179261}{x_1} - 2.5x_2 + \frac{66426}{x_2} - 16.4x_3 - \frac{12950295}{x_3} - 136.2x_4 - \frac{205520}{x_4} + 425.7x_5 - \frac{4571060}{x_5} - 1755.7x_6 - \frac{3066973}{x_6} + 98x_7 + \frac{3081814}{x_7} \quad (39)$$

#### 3.1.8.2 Linear with type two -Inverse mixed equation based model

$$f_{14}(x) = b_0 + b_1x_1 + \frac{b_2}{x_1} + b_3x_2 + \frac{b_4}{x_2} + b_5x_3 + \frac{b_6}{x_3} + b_7x_4 + \frac{b_8}{x_4} + b_9x_5 + \frac{b_{10}}{x_5} + b_{11}x_6 + \frac{b_{12}}{x_6} + b_{13}x_7 + \frac{b_{14}}{x_7} + b_{15}x_1x_2x_3x_4x_5x_6x_7 \quad (40)$$

$$f_{cm} = 2582041 - 0.313x_1 - \frac{336458}{x_1} + 0.491x_2 + \frac{380176}{x_2} + 1.038x_3 + \frac{169.384}{x_3} + 0.101x_4 - \frac{0.098}{x_4} - 5.82x_5 - \frac{145499}{x_5} - 30718.6x_6 - \frac{53080345}{x_6} + 0.13x_7 + \frac{0.221}{x_7} + 7.739 \times 10^{-13}x_1x_2x_3x_4x_5x_6x_7 \quad (41)$$

$$Slm = -8488691 - 1352x_1 + \frac{5262900}{x_1} + 1623x_2 + \frac{1842530}{x_2} - 5.67x_3 + \frac{1578091}{x_3} + 57378x_4 + \frac{86912006}{x_4} - 3879.5x_5 + \frac{43068132}{x_5} + 27900x_6 + \frac{48325462}{x_6} - 4058.2x_7 + \frac{10252898}{x_7} + 3.588 \times 10^{-13}x_1x_2x_3x_4x_5x_6x_7 \quad (42)$$

### 3.1.9 Sinusoidal equation based model

$$f_{15}(x) = b_0 + b_1 \sin x_1 + b_2 \sin x_2 + b_3 \sin x_3 + b_4 \sin x_4 + b_5 \sin x_5 + b_6 \sin x_6 + b_7 \sin x_7 \quad (43)$$

$$f_{cm} = 38.68 + 3.145 \sin x_1 - 3.365 \sin x_2 - 61.775 \sin x_3 + 3.90 \sin x_4 - 10 \sin x_5 - 87.62 \sin x_6 + 18.61 \sin x_7 \quad (44)$$

$$Slm = 492.2 + 43.5 \sin x_1 - 6.9 \sin x_2 + 83.5 \sin x_3 - 1.1 \sin x_4 - 0.042 \sin x_5 + 278.88 \sin x_6 + 7.65 \sin x_7 \quad (45)$$

### 3.1.10 Cosine equation based model

$$f_{16}(x) = b_0 + b_1 \cos x_1 + b_2 \cos x_2 + b_3 \cos x_3 + b_4 \cos x_4 + b_5 \cos x_5 + b_6 \cos x_6 + b_7 \cos x_7 \quad (46)$$

$$f_{cm} = 38.68 - 3.145 \cos x_1 - 3.365 \cos x_2 - 61.775 \cos x_3 + 3.9 \cos x_4 - 10 \cos x_5 - 87.62 \cos x_6 + 18.61 \cos x_7 \quad (47)$$

$$Slm = 492.2 + 43.5 \cos x_1 - 6.9 \cos x_2 + 83.5 \cos x_3 - 1.1 \cos x_4 - 0.042 \cos x_5 + 278.88 \cos x_6 + 7.65 \cos x_7 \quad (48)$$

## 4. Results and discussion

In this research, the mixture proportioning as given in Table 1 and test results of the 53 concrete mixes as shown in Figs. 1 and 2, were used to derive statistical models for estimating 28-day compressive strength, and slump flow of UHPC. Proper mathematical models were developed for the 28-day compressive strength, and the slump flow as functions of mix proportions. The sixteen mathematical models for each of responses (compressive strength and slump flow) were evaluated and examined based on their statistical characteristics.

### 4.1 Characteristics of models

Generally, error is made in prediction models due to limiting and scattering of existing data. Therefore, the error percentage of the models should be specified and evaluated. In the present study, the error percentage of different models for each mix design (as given in Table 1) is determined by Eq. 49. The maximum of these values are shown in Figs. 3 and 4 for the slump flow and the 28-day compressive strength, respectively.

Based on a comparison among the error values of the proposed slump flow equations, as shown in Fig. 3, it was observed that the error% value of slump flow Inverse-type 2 regression model (Eq. (12)) was lower than the other fifteen models. Therefore, this model (Eq. (12)) showed the best relation to the experimental observation for predicting the slump flow of UHPC, whereas the slump flow Power-type 3 regression model (Eq. (24)) presented the greatest values of error%, consequently, this model showed the least relation to the experimental observation for predicting the slump flow of UHPC. Thus, the slump flow Inverse-type 2 regression model (Eq. (12)) was the well-related model with the highest accuracy among the studying sixteen models to represent the UHPC slump flow. The other models also excellently describe the slump flow development pattern.

Also, by comparing among the error values of the proposed 28-day compressive strength

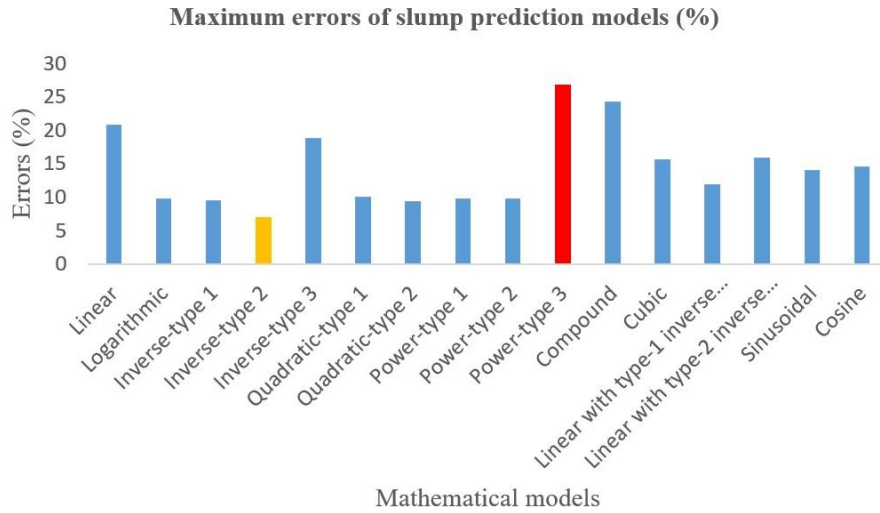


Fig. 3 Maximum errors of slump flow prediction models (%)

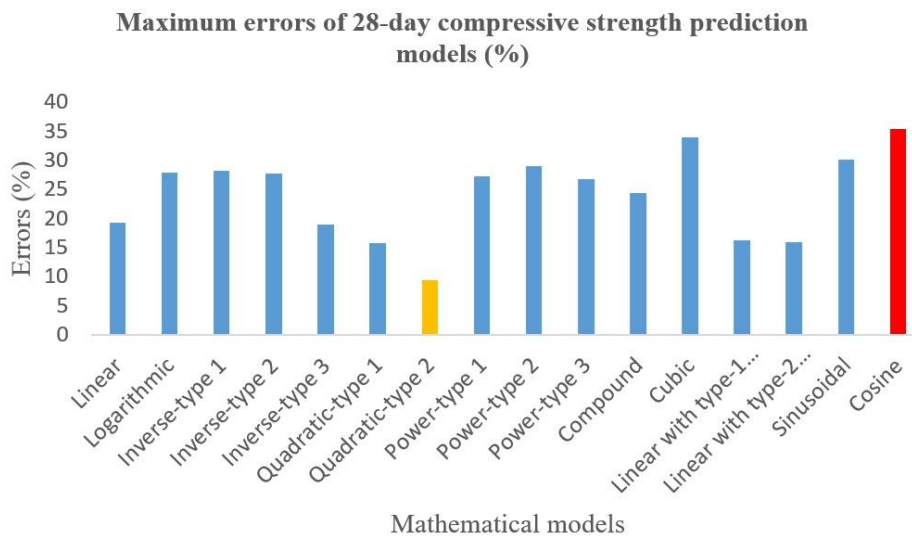


Fig. 4 Maximum errors of 28-day compressive strength prediction models (%)

equations, as shown in Fig. 4, it can be concluded that the error% value of compressive strength Quadratic-type 2 regression model (Eq. (32)) was lower than the other fifteen models. Therefore, this model (Eq. (32)) showed the best relation to the experimental observation for predicting the 28-day compressive strength of UHPC, whereas the compressive strength Cosine regression model (Eq. (47)) presented the greatest values of error%, consequently, this model showed the least relation to the experimental observation for predicting the 28-day compressive strength of UHPC. Thus, the compressive strength Quadratic-type 2 regression model (Eq. (32)) was the well-related model with the highest accuracy among the studying sixteen models to represent the UHPC 28-day compressive strength. The other models also excellently describe the compressive strength development pattern.

Table 2 Comparative analysis of slump flow models

Slump flow Regression Models	$R^2$
Eq. (3)	0.61
Eq. (6)	0.95
Eq. (9)	0.96
Eq. (12)	0.97
Eq. (15)	0.96
Eq. (18)	0.95
Eq. (21)	0.95
Eq. (24)	0.83
Eq. (27)	0.62
Eq. (30)	0.83
Eq. (33)	0.86
Eq. (36)	0.83
Eq. (39)	0.96
Eq. (42)	0.96
Eq. (45)	0.52
Eq. (48)	0.69

#### 4.2 Correlation of models

In order to evaluate the UHPC slump flow and 28-day compressive strength models correlation statistically,  $R^2$  values were measured. The values of  $R^2$  for the 16 mathematical models of UHPC slump flow are presented in Table 2. From this Table, the slump flow regression models can be ordered from least to greatest  $R^2$  values as follows: Eq. (45), Eq. (3), Eq. (27), Eq. (48), Eq. (24), Eq. (30), Eq. (36), Eq. (33), Eq. (6), Eq. (18), Eq. (21), Eq. (9), Eq. (15), Eq. (39), Eq. (42), and Eq. (12), which they are in the range between 0.52 to 0.97. In general, the proposed models have desired results. Therefore, according to the demanded accuracy, the proper model can be used with the appropriate number of terms. Based on comparison between the proposed equations, it was observed that  $R^2$  value of the slump flow Inverse-type 2 regression model (Eq. (12)) was greater than the other fifteen models. Therefore, this model (Eq. (12)) showed the best correlation to the experimental observation for predicting the UHPC slump flow, whereas the slump flow sinusoidal regression model (Eq. (45)) presented the lowest value of  $R^2$ , consequently, this model showed the worst correlation to the experimental observation for predicting the UHPC slump flow. Accordingly, slump flow Inverse-type 2 regression model (Eq. (12)) was the well correlated model with the highest accuracy among the studied sixteen models to represent the UHPC slump flow. The other models also describe the slump flow development pattern properly.

In addition, the values of  $R^2$  for the sixteen mathematical models of UHPC 28-day compressive strength are presented in Table 3. From this Table, the 28-day compressive strength regression models can be ordered from least to greatest  $R^2$  values as follows: Eq. (35), Eq. (17), Eq. (23), Eq. (5), Eq. (8), Eq. (44), Eq. (47), Eq. (20), Eq. (11), Eq. (14), Eq. (26), Eq. (2), Eq. (38), Eq. (41), Eq. (29), and Eq. (32), which they are in the range between 0.69 to 0.92. This indicates a good fit of the regression equations to the observations. However, the performance of the slump flow

Table 3 Comparative analysis of 28-day compressive strength models

Compressive Strength Regression Models	$R^2$
Eq. (2)	0.82
Eq. (5)	0.75
Eq. (8)	0.75
Eq. (11)	0.78
Eq. (14)	0.8
Eq. (17)	0.74
Eq. (20)	0.77
Eq. (23)	0.74
Eq. (26)	0.81
Eq. (29)	0.9
Eq. (32)	0.92
Eq. (35)	0.69
Eq. (38)	0.85
Eq. (41)	0.86
Eq. (44)	0.75
Eq. (47)	0.75

relations is better than the compressive strength relations. In general, the proposed models have great results. Therefore, according to the demanded accuracy, the proper model can be used with the appropriate number of terms. In other words, the other models may be used to their simplicity, despite their lower correlation. Also, it was found that the Quadratic-type 1, and 2 compressive strength models (Eq. (29) and (32)) are more suitable than other models. However, the Quadratic-type 2 model (Eq. (32)) represents the best fit to the experimental data. Therefore, this model (Eq. (32)) showed the best correlation to the experimental observation for predicting the 28-day compressive strength of UHPC, whereas the Cubic compressive strength model (Eq. (35)) presented the lowest value of  $R^2$ , consequently, this model showed the least correlation to the experimental observation for predicting the 28-day compressive strength of UHPC. Accordingly, the Quadratic-type 2 compressive strength regression model (Eq. (32)) was the well correlated model with the highest accuracy among the studied sixteen models to represent the 28-day compressive strength of UHPC. The other models also describe the compressive strength development pattern excellently.

## 5. Validation of the proposed models

The accuracy of the proposed models is validated by comparing obtained results with those from the literature (Ghafari *et al.* 2015). The result indicated that the Inverse-type 2 slump flow model, and the Quadratic-type 2 compressive strength model can obtain a better prediction of the ultra-high performance concrete properties. These models are also much faster at solving problems. Therefore, the proposed mathematical models can provide an efficient and accurate tool to predict and design UHPC.

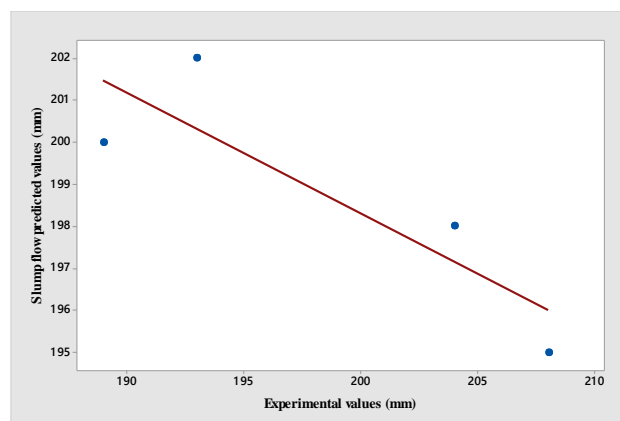
The comparison among the experimental data as given in Table 4, and the results of proposed prediction models are presented in Table 5, where it is shown that the maximum differences of

Table 4 Mixtures for the proposed criteria (Ghafari *et al.* 2015)

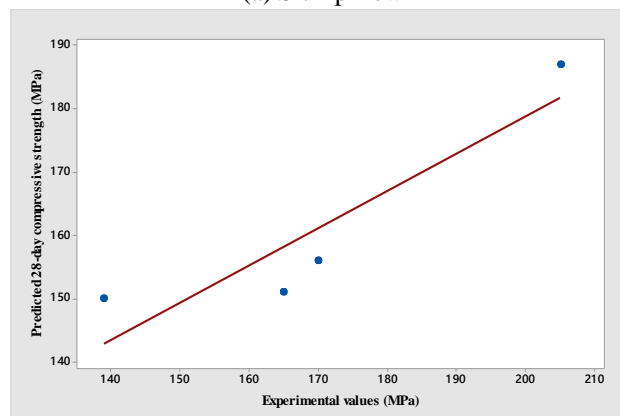
Mix Design	Constituents and Responses								
	Cement (Kg/m <sup>3</sup> )	Sand (Kg/m <sup>3</sup> )	Silica fume (Kg/m <sup>3</sup> )	Quartz flour (Kg/m <sup>3</sup> )	Water (Kg/m <sup>3</sup> )	Super plasticizer (Kg/m <sup>3</sup> )	Steel fibers (Kg/m <sup>3</sup> )	28-day Compressive strength (MPa)	Slump flow (mm)
N1	669	924	134	282	187	33	90	151	200
N2	673	920	132	281	190	30	98	156	195
N3	675	984	210	167	183	31	30	150	198
N4	729	868	193	211	191	30	113	187	202

Table 5 Predicted responses by model versus experimental measurement

Mix Design	Slump flow (mm)			28-day Compressive strength (MPa)		
	Experimental value	Predicted value	Difference (%)	Experimental value	Predicted value	Difference (%)
N1	200	189	5.5	151	165	-9.3
N2	195	208	-6.7	156	170	-8.97
N3	198	204	-3.03	150	139	7.3
N4	202	193	4.5	187	205	-9.6



(a) Slump flow



(b) 28-day Compressive strength

Fig. 5 Comparison between actual and predicted values: (a) Slump flow, (b) 28-day Compressive strength

6.7%, and 9.6% exist in slump flow, and 28-day compressive strength, respectively. Moreover, the difference between actual and predicted values was given in Fig. 5. In Fig. 5 and approved by the findings of Table 5, the results obtained from the proposed prediction models are in agreement with those of the experimental values.

## 6. Conclusions

In this study, sixteen mathematical models were developed and evaluated to predict the slump flow, and 28-day compressive strength of UHPC. The experimental results were used to develop the models. To obtain these results, several mixes with different water/cement ratios, silica fume, quartz flour, superplasticizer and steel fibers quantities were made and tested. Some important results of the study are as follows:

- 1) The Inverse-type 2 equation based model (Eq. (12)) was the well correlated model with the highest accuracy and the minimum error percentage among the other models to predict the slump flow of UHPC.
- 2) The Quadratic-type 2 equation based model (Eq. (32)) was the well correlated model with the highest accuracy and the minimum error percentage among the other models to predict the 28-day compressive strength of UHPC.
- 3) Slump flow Power-type 3 regression model (Eq. (24)), and the 28-day compressive strength Cosine regression model (Eq. (47)) presented the maximum error percentages, consequently, these models showed the worst prediction to the experimental observation for predicting the UHPC slump flow, and 28-day compressive strength, and their values were 26.8%, and 35.3%, respectively.

## References

- Abellán-García, J. (2020), "Four-layer perceptron approach for strength prediction of UHPC", *Constr. Build. Mater.*, **256**, 119465. <https://doi.org/10.1016/j.conbuildmat.2020.119465>.
- ACI: 211.1-91 (2009), Standard Practice for Selecting Proportions for Normal, Heavyweight, and Mass Concrete, American Concrete Institute.
- Al-Shamiri, A.K., Kim, J.H., Yuan, T.F. and Yoon, Y.S. (2019), "Modeling the compressive strength of high-strength concrete: An extreme learning approach", *Constr. Build. Mater.*, **208**, 204-219. <https://doi.org/10.1016/j.conbuildmat.2019.02.165>.
- Bao, Y., Valipour, M., Meng, W., Khayat, K.H. and Chen, G. (2017), "Distributed fiber optic sensor-enhanced detection and prediction of shrinkage-induced delamination of ultra-high-performance concrete overlay", *Smart Mater. Struct.*, **26**(8), 085009. <https://doi.org/10.1088/1361-665X/aa71f4>
- Bui, D.K., Nguyen, T., Chou, J.S., Nguyen-Xuan, H. and Ngo, T.D. (2018), "A modified firefly algorithm-artificial neural network expert system for predicting compressive and tensile strength of high performance concrete", *Constr. Build. Mater.*, **180**, 320-333. <https://doi.org/10.1016/j.conbuildmat.2018.05.201>.
- Cheng, Z., Zhang, Q., Bao, Y., Deng, P., Weri, C. and Li, M. (2021), "Flexural behavior of corrugated steel-UHPC composite bridge decks", *Eng. Struct.*, **246**, 113066. <https://doi.org/10.1016/j.engstruct.2021.113066>.
- Dao, D.V., Adeli, H., Ly, H.B., Le, L.M., Le, V.M., Le, T.T. and Pham, B.T. (2020), "A sensitivity and robustness analysis of GPR and ANN for high-performance concrete compressive strength prediction using a Monte Carlo simulation", *Sustain.*, **12**(3), 830. <https://doi.org/10.3390/su12030830>.

- Du, J., Meng, W., Khayat, K.H., Bao, Y., Guo, P., Lyu, Z., Abu-obeidah, A., Nassif, H. and Wang, H. (2021), "New development of ultra-high-performance concrete (UHPC)", *Compos. Part B: Eng.*, **224**, 109220. <https://doi.org/10.1016/j.compositesb.2021.109220>.
- Farzad, M., Shafieifar, M. and azizinamini, A. (2019), "Experimental and numerical study on bond strength between conventional concrete and ultra-high performance concrete", *Eng. Struct.*, **186**, 297-305. <https://doi.org/10.1016/j.engstruct.2019.02.030>.
- Ghafari, E., Bandarabadi, M., Costa, H. and Julio, E. (2015), "Prediction of fresh and hardened state properties of UHPC: comparative study of statistical mixture design and an artificial neural network model", *Mater. Civil Eng.*, **27**, 04015017. [https://doi.org/10.1061/\(ASCE\)MT.1943-5533.0001270](https://doi.org/10.1061/(ASCE)MT.1943-5533.0001270).
- Ghafari, E., Costa, H. and Julio, E. (2015), "Statistical mixture design approach for eco-efficient UHPC", *Cement Concrete Compos.*, **55**, 17-25. <https://doi.org/10.1016/j.cemconcom.2014.07.016>.
- Guo, P., Meng, W. and Bao, Y. (2021), "Automatic identification and quantification of dense microcracks in high-performance fiber-reinforced cementitious composites through deep learning-based computer vision", *Cement Concrete Res.*, **148**, 106532. <https://doi.org/10.1016/j.cemconres.2021.106532>.
- Khayat, K.H., Meng, W., Vallurupalli, K. and Teng, L. (2019), "Rheological properties of ultra-high performance concrete-An overview", *Cement Concrete Res.*, **124**, 105828. <https://doi.org/10.1016/j.cemconres.2019.105828>.
- Liu, J., Wu, C., Su, Y., Li, J., Shao, R., Chen, G. and Liu, Z. (2018), "Experimental and numerical studies of ultra-high performance concrete targets against high-velocity projectile impacts", *Eng. Struct.*, **173**, 166-179. <https://doi.org/10.1016/j.engstruct.2018.06.098>.
- Liu, Y., Zhang, Q., Meng, W., Bao, Y. and Bu, Y. (2019), "Transverse fatigue behavior of steel-UHPC composite deck with large-size U-ribs", *Eng. Struct.*, **180**, 388-399. <https://doi.org/10.1016/j.engstruct.2018.11.057>.
- Meng, W., Khayat, K.H. and Bao, Y. (2018), "Flexural behaviors of fiber-reinforced polymer fabric reinforced ultra-high-performance concrete panels", *Cement Concrete Compos.*, **93**, 43-53. <https://doi.org/10.1016/j.cemconcomp.2018.06.012>.
- Meng, W., Valipour, M. and Khayat, KH. (2016), "Optimization and performance of cost-effective ultra-high performance concrete", *Mater. Struct.*, **50**(1), 29. <https://doi.org/10.1617/s11527-016-0896-3>.
- Nguyen, N.H., Abellán-García, J., Lee, S. and Vo, T.P. (2024), "From machine learning to semi-empirical formulas for estimating compressive strength of Ultra-High Performance Concrete", *Exp. Syst. Appl.*, **237**, 121456. <https://doi.org/10.1016/j.eswa.2023.121456>.
- Qi, J., Cheng, Z., Zhou, K., Zhu, Y., Wang, J. and Bao, Y. (2021), "Experimental and theoretical investigations of UHPC-NC composite slabs subjected to punching Shear-flexural failure", *Build. Eng.*, **44**, 102662. <https://doi.org/10.1016/j.jobe.2021.102662>.
- Qu, D., Cai, X. and Chang, W. (2018), "Evaluating the effects of steel fibers on mechanical properties of ultra-high performance concrete using artificial neural networks", *Appl. Sci.*, **8**, 1120. <https://doi.org/10.3390/app8071120>.
- Regalwar, K., Heard, W.F., Williams, B.A., Kumar, D. and Ranade, R. (2020), "On enhancing mechanical behavior of ultra-high performance concrete through multi-scale fiber reinforcement", *Cement Concrete Compos.*, **105**, 103422. <https://doi.org/10.1016/j.cemconcomp.2019.103422>.
- Wang, J., Liu, J., Wang, Z., Liu, T. and Zhang, J. (2021), "Cost-effective UHPC for accelerated bridge construction: material properties, structural elements, and structural applications", *Bridge Eng.*, **26**, 04020117. [https://doi.org/10.1061/\(ASCE\)BE.1943-5592.0001660](https://doi.org/10.1061/(ASCE)BE.1943-5592.0001660).
- Wu, Z., Khayat, K.H. and Shi, C. (2019), "Changes in rheology and mechanical properties of ultra-high performance concrete with silica fume content", *Cement Concrete Res.*, **123**, 105786. <https://doi.org/10.1016/j.cemconres.2019.105786>.
- Wu, Z., Shi, C. and Khayat, K.H. (2019), "Investigation of mechanical properties and shrinkage of ultra-high performance concrete: Influence of steel fiber content and shape", *Compos. Part B: Eng.*, **174**, 107021. <https://doi.org/10.1016/j.compositesb.2019.107021>.
- Yin, H., Teo, W. and Shirai, K. (2017), "Experimental investigation on the behavior of reinforced concrete slabs strengthened with ultra-high performance concrete", *Constr. Build. Mater.*, **155**, 463-474.

<https://doi.org/10.1016/j.conbuildmat.2017.08.077>.

Zmetra, K.M., McMullen, K.F., Zaghi, A.E. and Wille, K. (2017), "Experimental study of UHPC repair for corrosion-damaged steel girder ends", *Bridge Eng.*, **22**(8), 04017037.  
[https://doi.org/10.1061/\(ASCE\)BE.1943-5592.0001067](https://doi.org/10.1061/(ASCE)BE.1943-5592.0001067).